Numerical Investigation for the Behaviour of Corrugated Steel Compact I-Section

Zinah K. Hasan [a]*, Sadjad A. Hemzah [a], Muslim Abdul- Ameer Al-Kannoon [b]

[a] Civil Engineering Department, Kerbala University, Karbala, Iraq
[b] Civil Engineering Department, Kufa University, Kufa, Iraq
* Corresponding author, Email: zinah.k@s.uokerbala.edu.iq

Abstract

The aim of the present work is to examine numerically the structural behavior of steel compact I-section with different corrugation technique. The experimental results of the ultimate strengths and deflection of one flat plate and eleven corrugated steel I-section investigated experimentally by the authors were used to validate the accuracy of the finite element results obtained from Abaqus F.E. program. Some parameters, like web corrugation width and core corrugation technique, were also examined. Results of finite element analysis showed a very good agreement with the those of experimental ones through the ultimate load and maximum displacement convergence. It was ensured from F.E. results that increasing flange corrugation height by ratio by 13% of web height increase the ultimate load by about 27% with little decrease in vertical deformation. Also, it was insured that failure mode for most specimens changed from flexural failure to shear failure. Furthermore, the effect of web corrugation width and changing flange core corrugation from inclined to vertical direction decrease both ultimate load and deflection of analyzed specimens [1].

Keywords: Steel; ABAQUS; Numerical study; Flange corrugation; Compact section.

1. Introduction

Many researchers mentioned the finite product in their research. Chan et al., 2002 [2] Use the finite element technique to find the influence of web corrugation on the bending potential of the beam, beams were studied with plan web, horizontally corrugated web, and vertically corrugated web. Half circle corrugation is the corrugation profiles surveyed. The corrugation radius has also been investigated;

it has been found that the corrugated web beams have a higher corrugation radius, means that it will be capable of maintaining a higher bending moment. While vertical corrugated web displayed a higher flexural moment capability improvement compared to the horizontal forms by about (38% to 54%). The vertically corrugated web also results in stronger protection against the flange's buckling. In contrast to the flat web beam, it has also been found that vertically corrugated beams have a 10.60 % weight increment. Moon et al., 2009 [3] presented results of numerical analysis of finite elements of the lateral-torsional buckling of beams with the corrugated webs which are under the uniform bending. Previous studies on the torsional and bending stiffness of the beam with the corrugated webs have been discussed, then approximate approaches are proposed for determining the center of the shear and computing the warping constant. Utilizing the suggested approaches, the lateral-torsional buckling strength of the beam with corrugated webs under uniform bending may be computed easily. According to the results, it has been discovered that the warping constants of the beam with corrugated webs were greater compared to those of flat web beams. The authors found that the elastomeric sideways twisting force increased by 10% with the increase in the corrugation angle of the corrugated web. Alinia et al., 2009[4] examine the shear failure mechanism, a three-dimensional analysis was presented using the (ABAQUS) finite element system of full-on full scale steel plate girders. The main objective of the study is to understand why and how in laboratory experiments plastic hinges were formed, it was found that shear-induced plastic hinges only occur in the flanges of end panels after developing partially inclined yield zones in the webs. They do not exist in the middle panels, furthermore, plastic hinges are shaped due to the shear deformation of the girders, directly related to stiffness related to end posts as well as flange dimensions. The position of the plastic hinges is not specifically associated with stresses exerted by inclined fields of tension. The experimental program of Marwan Ahmed, Haider K. Ammash., 2020 [5] involved testing ten simply supported steel beams, having the same weight and different geometrical properties. The study focused on the load-deflection behavior and the overall shear behavior, The obtained results of the finite element analysis using ABAQUS software were compared with the experimental results of all beams tested. The comparison is presented in the expression of the ultimate load, ultimate deflection, load-deflection curve, and the deformed shape. The finite element models gave the same shape and location of the deformation at failure for all girders as experimental work.

Ibtihal Adnan Suhail, Muslim Abdual- Ameer Khodair, 2020[6] tested six groups of simply supported steel beams in their experimental program, each group consists of two beams with total number of tested beams of twelve simply supported beam. A three-dimensional finite elements analysis of the specimens

using ANSYS 14.5 software is presented. In order to verify the analysis validity for steel beams with various profiles of corrugated web accuracy, the numerical method was checked through comparing experimental results at yielding and failure loads, load-deflection curves and stress distribution with the F.E analysis. The finite element model showed a good accuracy in analyzing corrugated steel web beams. The predicted yielding and ultimate loads, in addition the total flexural behavior had a good matching with respect to the experimental result.

Creation of a numerical model based on data obtained from an under-publishing paper carried out by the authors [1] is the aims to of this study. Also, some other parameters, like web corrugation width and core corrugation technique, were also numerically examined through finite element analysis program (Abaqus). The geometric and section properties of the steel plates used to form experimentally examined specimens are shown in Figure (1) and Table (1), while material properties of used steel plates are listed in table (2). All tested specimens were simply supported under the action of two applied force concentrated at distance one third from supports.
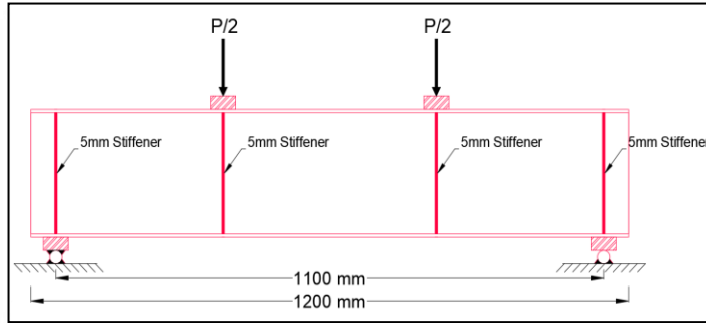
a) **Overall specimen geometry**
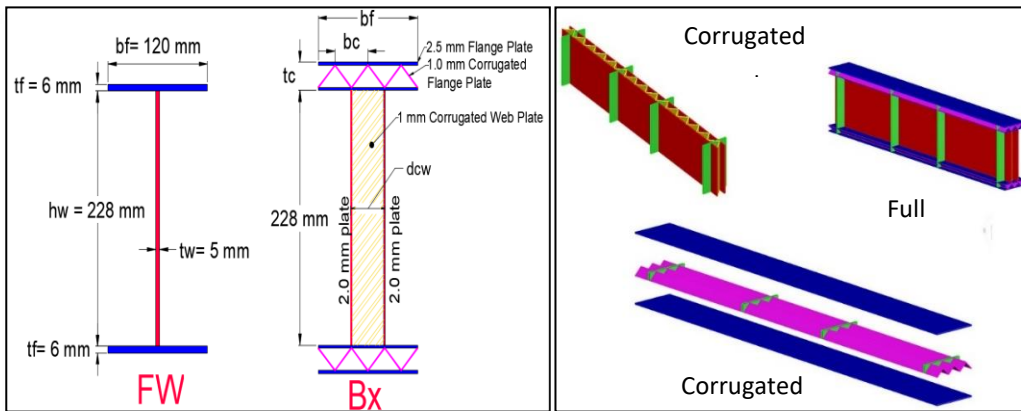
b) **Cross-section details**   c) **Overall geometry**

Figure 1 Specimen's geometry and section details

Table 1 Dimensions of tested specimens

Group	Identificat-ion	Bf	Top flange					Bottom flange					Web				bc/dcw
			tf	ts	tc	dc	bc	tf	ts	tc	dc	bc	hw	tw	ts	tc	
G1	Standard	120	6	---	--	---	---	6	---	--	----	---	228	5	--	--	---
G2	C20WBT3	120	---	2.5	1	20	40	--	2.5	1	20	40	228	--	2	1	40
	C20WT3	120	--	2.5	1	20	40	6	---	--	----	----	228		2	1	40
	C20WB3	120	6	---	--	---	---	--	2.5	1	20	40	228	--	2	1	40
	C20WBT4	120	---	2.5	1	20	40		2.5	1	20	40	228	--	2	1	40
	C20BT3	120	---	2.5	1	20	40	--	2.5	1	20	40	228	5	--	--	---
G3	C30WBT3	120	---	2.5	1	30	40	--	2.5	1	30	40	228	--	2	1	40
	C30BT3	120	---	2.5	1	30	40	--	2.5	1	30	40	228	5	--	--	---
G4	C35WBT3	120	---	2.5	1	35	40	--	2.5	1	35	40	228	--	2	1	40
	C35WT3	120	---	2.5	1	35	40	6	---	--	----	---	228	--	2	1	40
	C35WB3	120	6	---	--	---	---	--	2.5	1	35	40	228	--	2	1	40
	C35T3	120	---	2.5	1	35	40	6	--	--	----	----	228	5	--	--	---

*All units are in mm

Table 2 Material properties of plates

Plate thickness t (mm)	Yield stress fy (MPa)	Ultimate stress fu (MPa)
6	335	487
5	342	460
2.5	272	310
2	253	297
1	238	285

2. Modelling plate material

The numerical study consists of simulating the experimental work, which involves one flat plate beam and eleven corrugated steel I-section beams. The entire materials in the modelling of these beams includes steel plates with two types of elements (brick element for supporting and loading plate and shell element for other specimens components.

Four steel plates modeled as a brick element, these plates were used at supports and under concentrated loads of the model with dimensions of (120×50×25) mm for length, width, and height, respectively. While plates which were used to form the steel section and stiffeners were modeled as shell element as shown in Figure (2). The elastic modulus and Poisson's ratios for all plates were assumed 200 GPa and 0.3, respectively. The plates were assembled and connected at all edges by tie constrain,
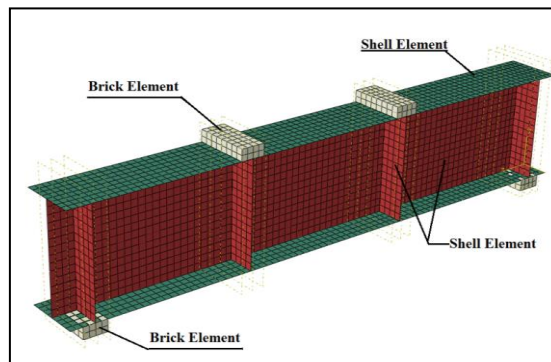
Figure 2 Abaqus model for control beam

3. Loading and Boundary Condition

To ensure the same behavior of the model to the same way as the experimental specimens boundary conditions, two steel plates have performed these loads at a distance (L/3) from the supports. Displacement of the boundary condition was utilized to constrain all specimens' models to get the

appropriate solution. All models were constrained in the z-direction and y-direction (Uz=Uy0=) at the hinge support at a distance of 50 mm from the end of the beam, while they were constrained in the y-direction and x-direction (Uy= Ux=0) at the roller support at a distance of 50 mm from the end of the beam, as illustrated in Figure (3).
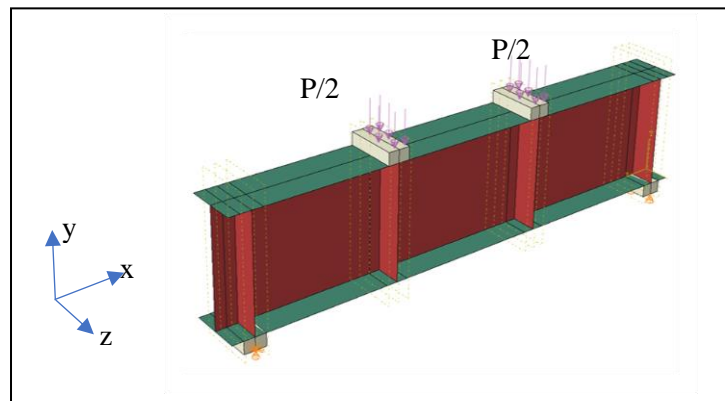
Figure 3 Applied loads and boundary conditions

4. Mesh Optimization

In finite element modeling, choosing the mesh size is crucial. Prior to the study, adequate pre-analysis of the various mesh densities was conducted to determine the optimum density to provide the necessary precision based on the analysis' complexity. When the beam is divided into a sufficient number of items, good convergence of results can be achieved. When reducing the mesh size had little impact on the performance, this was mostly accomplished.

Convergence studies were carried out on the flat web beam with various mesh densities, changing the total number of elements from 183 to 5450, and then plotting the mid-span deflection versus the number of elements as shown in Figure (4).
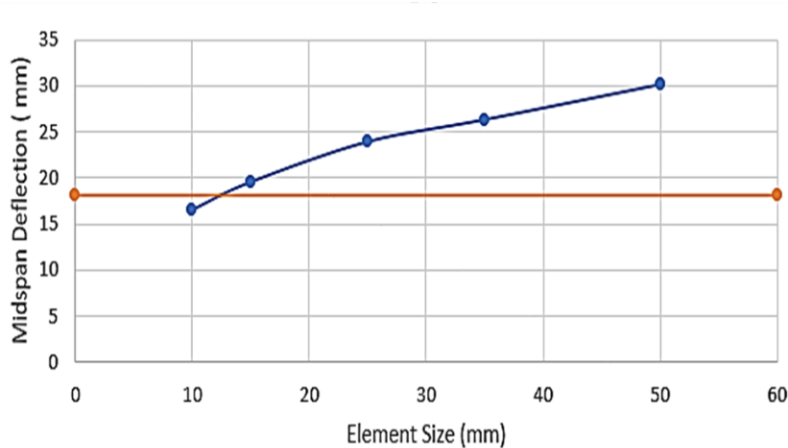
Figure 4 Convergence study curve

When the number of elements is greater than 3260, there is an unnoticeable difference in the mid-span deflection. As a result, in the verification analysis of the checked samples, the element size corresponding to this figure was adopted, which is equivalent to 20 mm.

5. Numerical analysis verification results and discussions

All specimens, flat plate and corrugated with different height and type (Table 1), were modelled and analyzed using Abaqus software. Figures 5 to (16) show a comparison between the experimental and the numerical results of load-vertical deflection curves, where the deflection is measured at the midspan center of the bottom face, and failure mode. The validity of numerical results can be obtained from these figures and listed in table (3), which showed a good convergence with the experimental results.

It's clearly noticed from figures and table (3) that difference in ultimate load ranged from -0.8% to 3.6%, also the difference in ultimate midspan deflection ranged from -5.9% to 18.4%. The difference in deflections may also be occurs due to technical errors in fixing the specimens or welding process.

Failure modes of all analyzed beams were identical with experimental ones. Which ensure the validity of the applied finite element analysis to be used for further specimens with different parameters.
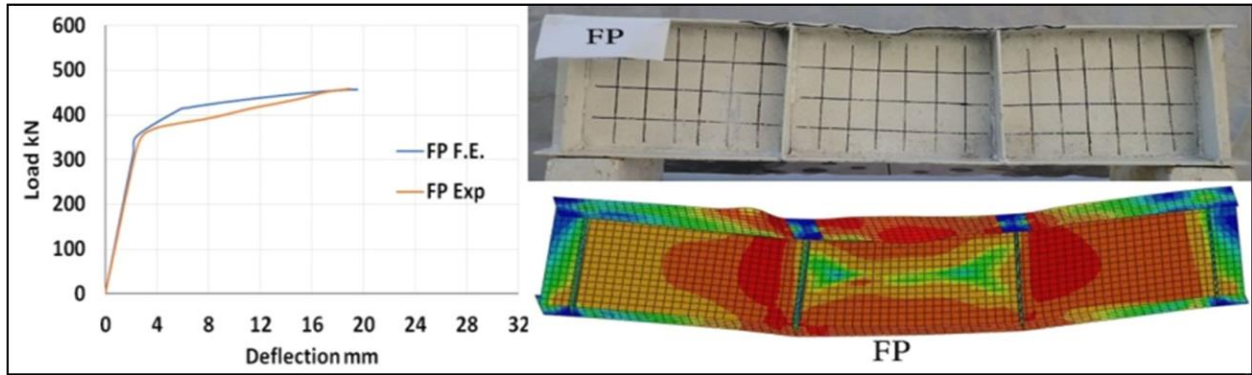
Figure 5 Experimental and numerical load-deflection curve and failure mode for F.P specimen
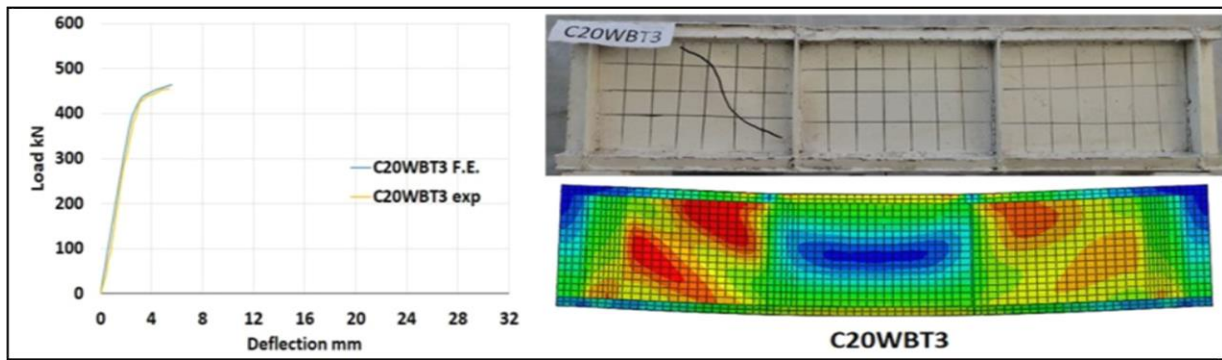
Figure 6 Experimental and numerical load-deflection curve and failure mode for C20WBT3 specimen
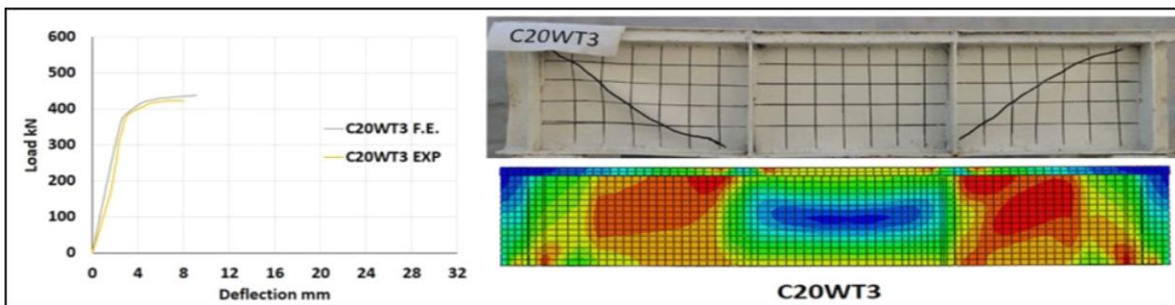
Figure 7 Experimental and numerical load-deflection curve and failure mode for C20WT3 specimen
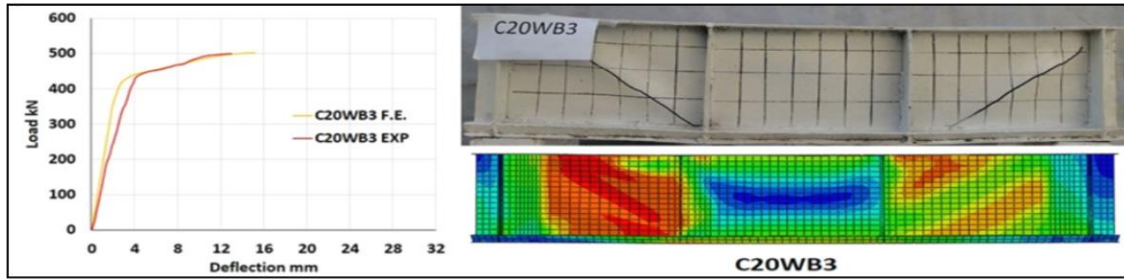
Figure 8 Experimental and numerical load-deflection curve and failure mode for C20WB3 specimen
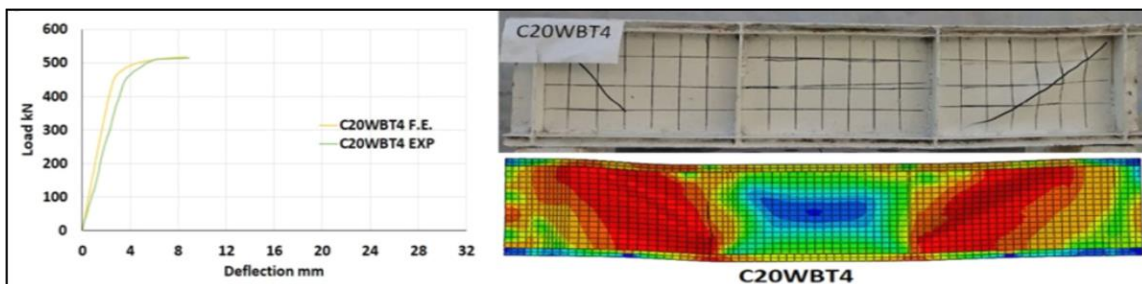
Figure 9 Experimental and numerical load-deflection curve and failure mode for C20WBT4 specimen
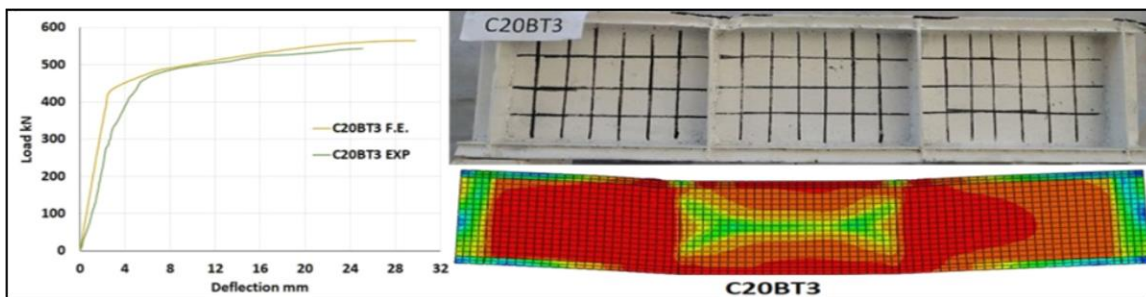
Figure 10 Experimental and numerical load-deflection curve and failure mode for C20BT3 specimen
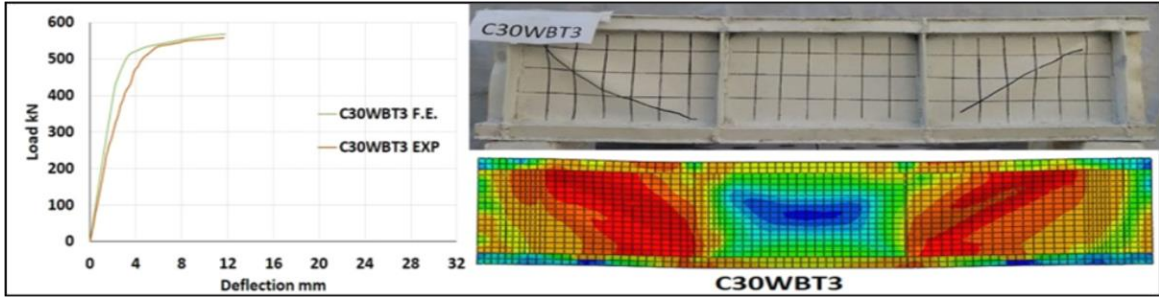
Figure 11 Experimental and numerical load-deflection curve and failure mode for C30WBT3 specimen plate
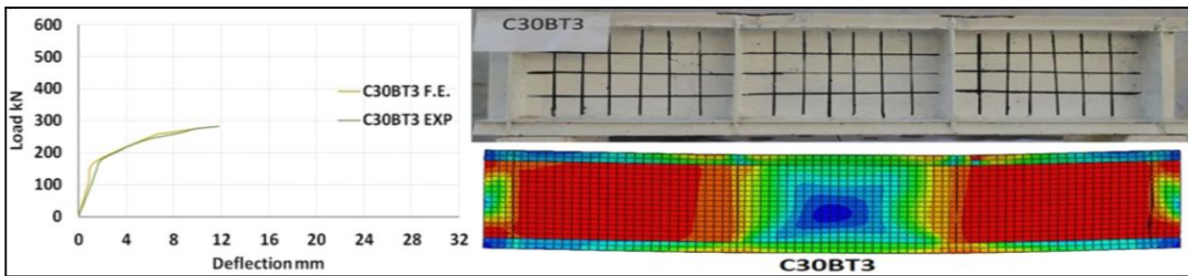
Figure 12 Experimental and numerical load-deflection curve and failure mode for C30BT3 specimen
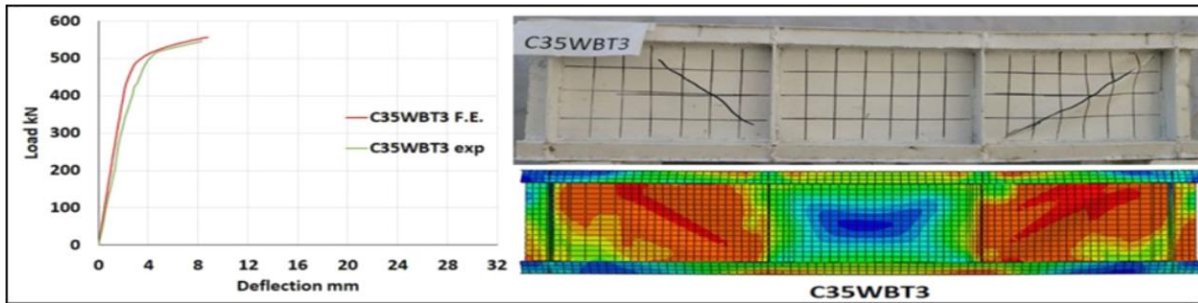
Figure 13 Experimental and numerical load-deflection curve and failure mode for C35WBT3 specimen
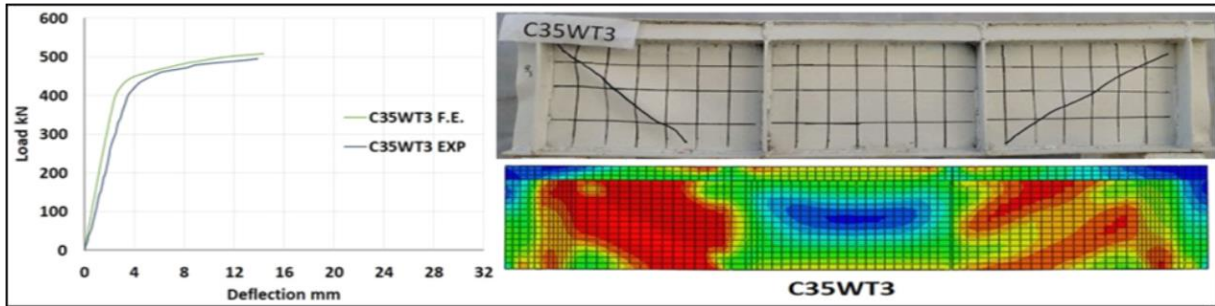
Figure 14 Failure shape of experimental and numerical and failure mode for C35WT3 specimens
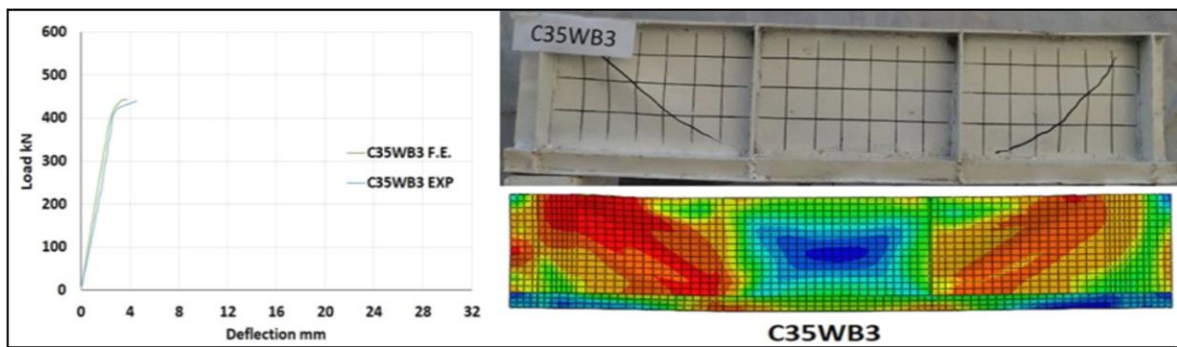
Figure 15 Experimental and numerical load-deflection curve and failure mode for C35WB3 specimen
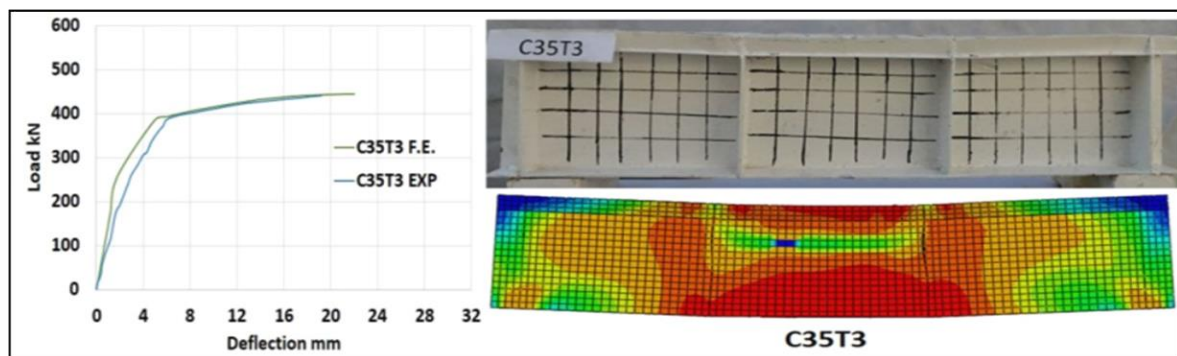
Figure 16 experimental and numerical load-deflection curve and failure mode for C35T3 specimen

Table 3 Experimental and Numerical Result for Tested Beams

Group	Space.	Ultimate Load (KN)			Ultimate deflection (mm)		
		EXP	F. E	Ratio%	EXP	F. E	Ratio%
G1	F. P	441	457.1	3.6%	18.1	19.5	7.7%
G2	C20WBT3	455	463.9	1.9%	5.4	5.5	1.8%
	C20WT3	424	438.6	3.4%	7.9	9.1	15.1%
	C20WB3	500	502.2	0.44%	13	15.1	16.1%
	C20WBT4	515	518.5	0.67%	8.9	8.7	-2.24%
	C20BT3	543	564.5	3.9%	25.08	29.7	18.4%
G3	C30WBT3	558	568.2	1.8%	11.7	11.7	0
	C30BT3	283	280.5	-0.8%	11.8	11.1	-5.9%
G4	C35WBT3	545	556.3	2.4%	8.3	8.7	4.8%
	C35WT3	495	508.2	2.6%	13.9	14.3	2.8%
	C35WB3	440	443.5	0.7%	4.55	3.7	-18.6%
	C35T3	441	444.5	0.79%	19.2	22	14.5%

6. Parametric Study

To examine the effect of some parameters on the behavior of corrugated steel beam under the effect of two concentrated loads, two parametric study was investigated by applying the numerical application by ABAQUS. The selected parameters included web corrugation width and flange core corrugation pattern.

6.1 Web Corrugation Width (C30W20BT3)

To examine the effect of corrugated web width on the behavior of corrugated steel beam under the effect of two concentrated loads, a 20 mm web width was modeled for specimen C30W20BT3 instead of 42 mm experimental width of beam C30WBT3. This change required to change the flange core corrugation to match web edges at intersection lines as shown in figure (17). It could be found that the ultimate load capacity and deflection of modified specimen is decreased to 538.9 kN and 5.4 mm respectively if compared with 568.3 kN and 11.8 mm of specimen C30WBT3 respectively. The failure mode was also changed from shear failure to flanged plus web buckling failure, Figure (18).
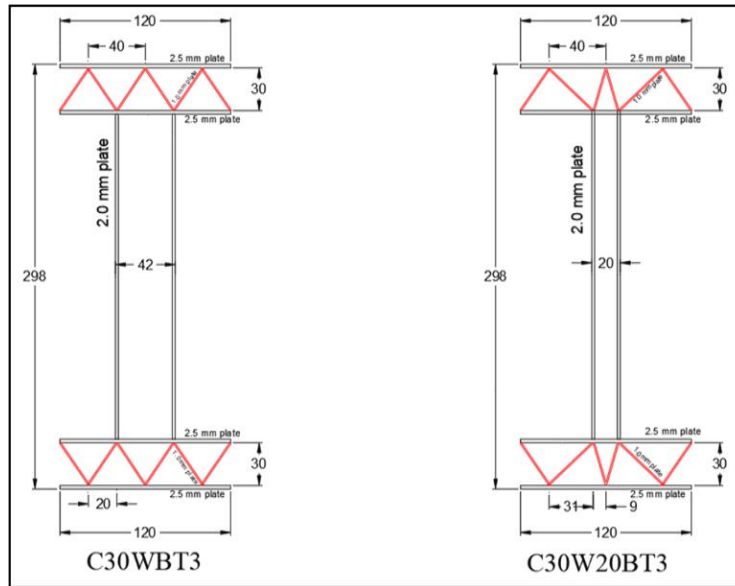
Figure 17 Beams C30WBT3 and C30W20BT3 section properties
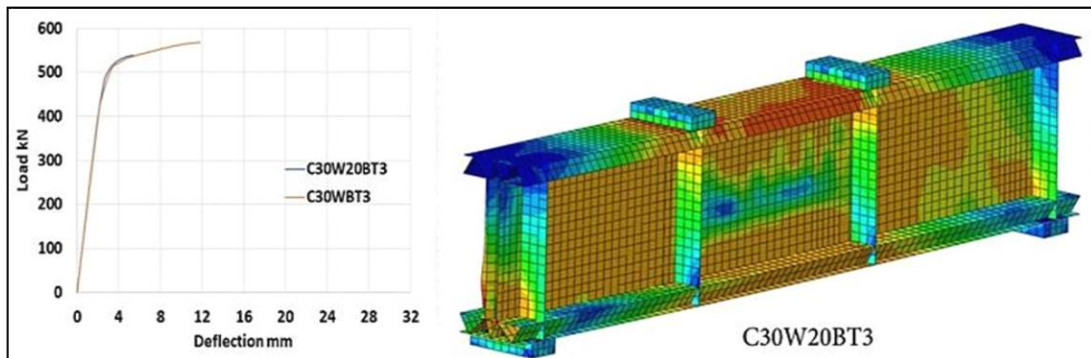
Figure 18 Load deflection curve and failure mode for specimens C30WBT3 and C30W20BT3

6.2 Flange Core Corrugation Pattern

Specimens C30WBT3 and C20BT3 were chosen to change the core corrugation from inclined to vertical direction. The new specimens were labeled as C30WBT3V and C20BT3V. The thickness of the core was kept to be 1 mm as well as other section properties as shown in Figure (19). It is obviously noted from Figures (20) and Figures (21) that both changed in core corrugation direction made a reduction in ultimate load capacity to 426.3 kN and 468.3 kN for beams C30WBT3V and C20BT3V respectively if compared with 568.3 kN and 564.6 kN for C30WBT3 and C20BT3 specimens. A

reduction in midspan deflection could be also noted for both specimens which reaches to 4.6 mm and 22.6 mm for specimens C30WBT3V and C20BT3V respectively, while C30WBT3 and C20BT3 had a deflection value of 11.8 mm and 29.8 mm respectively. However, flexural failure mode was recorded for new specimens while only C30WBT3 beam had a shear failure.
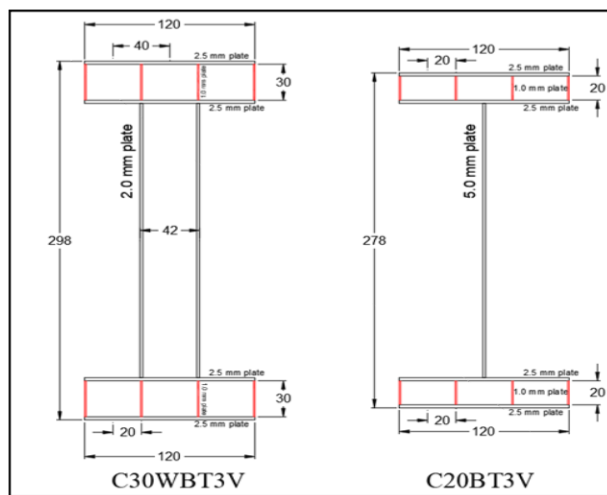
Figure 19 Beams C30WBT3V and C20BT3V section properties
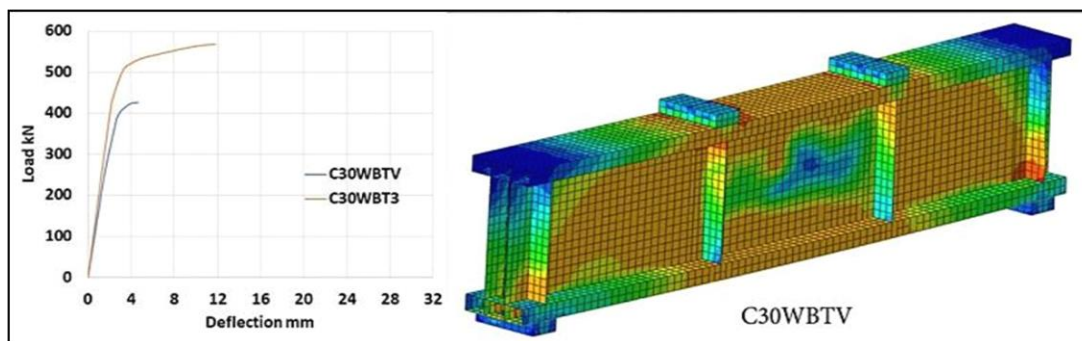
Figure 20 Load deflection curve and failure mode for specimens C30WBT3 and C30WBTV
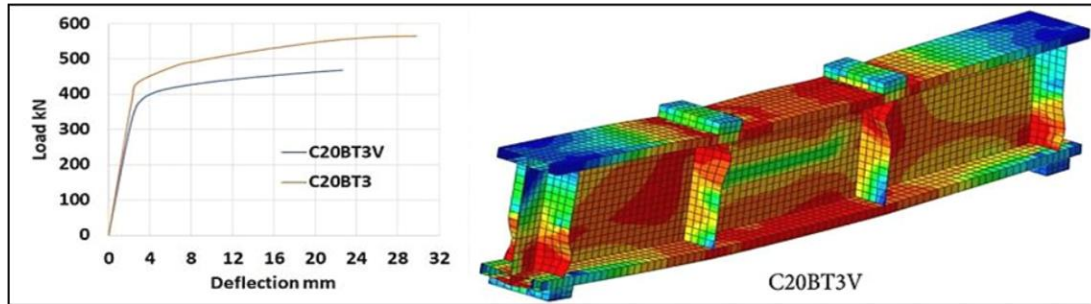
Figure 21 Load deflection curve and failure mode for specimens C20BT3V and C20BT3V

7. Conclusions

From the obtained numerical results of finite element analysis program (Abaqus), the following conclusions could be drawn:

1. The validity of the numerical solution could be ensured to analyze corrugated steel compact section based on maximum differences in ultimate load and midspan deflection of the tested specimens which ranged between 3.9% and 18.6% respectively.

2. Use of vertical core corrugation in flanges instead of inclined one will reduce ultimate load by about 24% and 17.6% and midspan deflection by 61% and 24%.

3. Use of vertical core corrugation may change the failure mode depending on flange corrugation height and web width.

4. Decreasing web width by 50% of original corrugated width makes a reduction in both ultimate load and deflection of tested specimen, also it will change the failure mode from shear to flexural failure which ensure that stresses were redistributed to be more concentrated on flanges.

REFERENCES

[1] Zinah K Hasan, Sadjad A Hemzah, Muslim Abdul- Ameer Khudhair Al-Kannoon "Behavior of Corrugated Steel Compact I-Section Beams" 2nd International Conference for Civil Engineering Science (2021), Journal of Physics, vol. 1895, no. 1.

[2] CL Chan, YA Khalid, BB Sahari, and AMS Hamouda, "Finite element analysis of corrugated web beams under bending," J. Constr. Steel Res., vol. 58, no. 11, pp. 1391–1406, 2002.

[3] J Moon, JW Yi, BH Choi, and HE Lee, "Lateral–torsional buckling of I-girder with corrugated webs under uniform bending," Thin-Walled Struct., vol. 47, no. 1, pp. 21–30, 2009

[4] MM Alinia, M Shakiba, and HR Habashi, "Shear failure characteristics of steel plate girders," Thin-Walled Struct., vol. 47, no. 12, pp. 1498–1506, 2009

[5] Marwan Ahmed, Haider K. Ammash, "Shear Behavior of Corrugated Core Webs for Steel Plate Girders", IOP Conf. Series: Materials Science and Engineering, vol. 1090, pp. 1–10,2021.

[6] Ibtihal Adnan Suhail, Muslim Abdual- Ameer Khudhair, " FLEXURAL BEHAVIOR OF STEEL BEAMS WITH CORRUGATED WEB", International Journal of Scientific & Technology Research, vol 8, no. 10, pp. 3004 – 3009, 2019.

التحري العددي لتصرف الأعتاب المموجة ذات المقاطع الحديدية المضغوطة

الخلاصة: الهدف من العمل الحالى هو فحص السلوك الهيكلى للصلب المصنع على شكل section-I بشكل عددى مع اختلاف تقنية التمويج. النتائج التجريبية للحمل الاقصى والتشوهات لنموذج مسطح واحد وأحد عشر نموذجا مموجا تم فحصخا من قبل الباحث تم استخدامها للتحقق من دقة النتائج المتحصلة من برنامج العناصر المحددة Abaqus. تم دراسة بعض المؤثرات مثل عرض تمويج الويب والتمويج الأساسى للشفة أيضًا. أظهرت نتائج تحليل العناصر المحددة توافقًا جيدًا جدًا مع النتائج التجريبية منها من خلال الحمل النهائى وتقارب الإزاحة القصــوى. تم التوصــل الى أن زيادة الحافة ارتفاع التموج بنســبة 13٪ من ارتفاع المقطع يزيد الحمل النهائى بحوالى 27٪ مع انخفاض طفيف فى التشوه الرأسى. ، أيضًا تم ملاحظة أن وضع الفشل لمعظم العينات قد تغير من فشل الانحناء إلى فشــل القص. علاوة على ذلك لوحظ ان تأثير عرض تمويج الويب وتغيير تمويج قلب الحافة من الاتجاه المائل إلى الاتجاه الرأســى ادى الى تقليل كل من الحمل النهائى وانحراف العينات التى تم تحليلها باستحدام برنامج العناصر المحددة Abaqus